

Implications of geometric plasticity for maximizing photosynthesis in branching corals

P. Kaniewska · K. R. N. Anthony · E. M. Sampayo ·
P. R. Campbell · O. Hoegh-Guldberg

Received: 21 May 2013 / Accepted: 24 September 2013 / Published online: 8 October 2013
© Springer-Verlag Berlin Heidelberg 2013

Abstract Reef-building corals are an example of plastic photosynthetic organisms that occupy environments of high spatiotemporal variations in incident irradiance. Many phototrophs use a range of photoacclimatory mechanisms to optimize light levels reaching the photosynthetic units within the cells. In this study, we set out to determine whether phenotypic plasticity in branching corals across light habitats optimizes potential light utilization and photosynthesis. In order to do this, we mapped incident light levels across coral surfaces in branching corals and measured the photosynthetic capacity across various within-colony surfaces. Based on the field data and modelled frequency distribution of within-colony surface light levels, our results show that branching corals are substantially self-shaded at both 5

and 18 m, and the modal light level for the within-colony surface is $50 \mu\text{mol photons m}^{-2} \text{s}^{-1}$. Light profiles across different locations showed that the lowest attenuation at both depths was found on the inner surface of the outermost branches, while the most self-shading surface was on the bottom side of these branches. In contrast, vertically extended branches in the central part of the colony showed no differences between the sides of branches. The photosynthetic activity at these coral surfaces confirmed that the outermost branches had the greatest change in sun- and shade-adapted surfaces; the inner surfaces had a 50 % greater relative maximum electron transport rate compared to the outer side of the outermost branches. This was further confirmed by sensitivity analysis, showing that branch position was the most influential parameter in estimating whole-colony relative electron transport rate (rETR). As a whole, shallow colonies have double the photosynthetic capacity compared to deep colonies. In terms of phenotypic plasticity potentially optimizing photosynthetic capacity, we found that at 18 m, the present coral colony morphology increased the whole-colony rETR, while at 5 m, the colony morphology decreased potential light utilization and photosynthetic output. This result of potential energy acquisition being underutilized in shallow, highly lit waters due to the shallow type morphology present may represent a trade-off between optimizing light capture and reducing light damage, as this type morphology can perhaps decrease long-term costs of and effect of photoinhibition. This may be an important strategy as opposed to adopting a type morphology, which results in an overall higher energetic acquisition. Conversely, it could also be that maximizing light utilization and potential photosynthetic output is more important in low-light habitats for *Acropora humilis*.

Communicated by R. Hill.

Electronic supplementary material The online version of this article (doi:10.1007/s00227-013-2336-z) contains supplementary material, which is available to authorized users.

P. Kaniewska · K. R. N. Anthony
Australian Institute of Marine Science, PMB 3, Townsville MC,
QLD 4810, Australia

P. Kaniewska (✉) · E. M. Sampayo
School of Biological Sciences, The University of Queensland,
St Lucia, QLD 4072, Australia
e-mail: p.kaniewska@aims.gov.au

P. R. Campbell
Department of Agriculture, Fisheries and Forestry, Dutton Park,
QLD 4102, Australia

O. Hoegh-Guldberg
Global Change Institute, ARC Centre of Excellence, The
University of Queensland, St Lucia, QLD 4072, Australia

Introduction

Many organisms occupy fluctuating environments at both spatial and temporal scales (Meyers and Bull 2002). Scleractinian corals are found across a wide range of environmental gradients for light (e.g. Anthony and Fabricius 2000; Anthony and Hoegh-Guldberg 2003a; Vermeij and Bak 2002), water flow (Bruno and Edmunds 1998; Kaandorp et al. 2005) and temperature (Achtuv and Dubinsky 1990; Kleypas et al. 1999). Corals have evolved a range of physiological (Brown et al. 2002; Fagoonee et al. 1999; Stimson 1997; Warner et al. 2002), behavioural (Levy et al. 2003) and morphological mechanisms (Anthony et al. 2005; Bruno and Edmunds 1997; Enriquez et al. 2005; Marcelino et al. 2013) to cope with environmental fluctuations. Morphological variation in reef-building corals is one of these examples whereby phenotypic plasticity, i.e. the change in physiological or morphological characteristics of a genotype (Bradshaw 1965), may confer an advantage in confronting environmental heterogeneity (Sultan et al. 2002; Via et al. 1995). While many corals display changes in colony geometry across environmental gradients (Bruno and Edmunds 1997; Willis 1985), it is unclear whether this relates to improvements in energy acquisition or is a mere result of growth limitations during development. Morphological variation in corals can result in similar levels of productivity across flow regime gradients (Lesser et al. 1994). In addition, changes in colony architecture can optimize within-colony surface irradiance across gradients in ambient light levels (Anthony et al. 2005; Kaniewska et al. 2008) and can facilitate energy acquisition (Hoogenboom et al. 2008).

Light has special significance to reef-building corals, given the dependence of these organisms on the symbiotic relationship between the coral host and photosynthetic dinoflagellates of the genus *Symbiodinium* (Muscatine and Porter 1977). Due to the photosynthetic component of the symbiosis, it is likely to confer an advantage whether ambient light regimes are adjusted to a photosynthetically optimum irradiance (Anthony and Hoegh-Guldberg 2003b; Enriquez et al. 2005; Hoogenboom et al. 2008). Photoacclimation is common in *Symbiodinium* in response to changes in light regimes (e.g. Dustan 1979; Iglesias-Prieto and Trench 1994); the symbiont can vary both the density and amount of photosynthetic pigments on a time scale from seconds to days (e.g. Iglesias-Prieto and Trench 1997; Titlyanov et al. 2002; Dove et al. 2008). In addition, there are host factors, which can help modulate ambient irradiance levels available to the coral and *Symbiodinium*, these include polyp contraction (Levy et al. 2003), skeletal structure (Enriquez et al. 2005; Stambler and Dubinsky 2005) and light absorption by fluorescent and non-fluorescent pigments (Dove 2004; Salih et al. 2000). Also, variations

in colony morphology can aid in manipulating and optimizing within-colony irradiance levels (Anthony et al. 2005; Kaniewska et al. 2008; Muko et al. 2000). Changes in the photophysiology of the symbiont is a flexible response, which can easily adapt to short-term changes (hours to days) in the ambient light environment, while the more permanent morphological changes in the coral colony shape can aid in providing an overall near-optimal within-colony light climate to facilitate the photoacclimatory response of the symbiont. These two mechanisms working in conjunction with each other can expand the host–symbiont complex's light niche (Hoogenboom et al. 2008).

Studies of photoacclimation have mainly focused on large-scale environmental variability such as bathometric differences (e.g. Battery and Porter 1989; Fricke et al. 1987; Graus and Macintyre 1976; Oliver et al. 1983). This assumes that the host–symbiont complex acts as a single unit with a homogenous response and that photoacclimation occurs mainly at the level of the symbiont. Several studies have shown that this may not necessarily be the case (Goulet and Coffroth 1997; Hoogenboom et al. 2006; Jokiel and Morrissey 1986). In fact, not only does colony morphology play a role in self-shading but within-tissue self-shading also significantly alters light levels reaching the *Symbiodinium* cells inside the host tissues (Kaniewska et al. 2011; Wangpraseurt et al. 2012). Structural self-shading in sea grasses results in photosynthetic variability along a leaf, which is comparable in magnitude to changes in photosynthetic performance along bathometric gradients (Enriquez et al. 2002). In corals, colony morphology may play an important part in creating within-colony niches of sun-exposed and sun-shaded areas (Kaniewska et al. 2008). The heterogeneous nature of light and water flow within a colony can result in variable photosynthetic capacity across entire colonies (Kuhl et al. 1995; Helmuth et al. 1997a) but also at smaller scales, within-colony differences at the corallite level have been documented (Hill et al. 2004; Wangpraseurt et al. 2012). However, to date, variable photosynthetic activity has not been mapped across an entire colony of a branching coral species, and a clear pattern of structural within-colony photosynthetic variation in relation to colony morphology remains to be described.

Currently, there is extensive information on physiological photoacclimatory mechanisms and their effects on photosynthetic performance in corals (e.g. Dove et al. 2006; Dubinsky et al. 1984). However, the significance of phenotypic plasticity across environmental light gradients is not well described. Variation in phenotypic plasticity among species can influence the size of their light niche and thereby affect species distribution limits (Meyers and Bull 2002). There is considerable morphological variation across light niches for *Acropora humilis*, where colonies have greater branch spacing and shorter branches in

deep, low-light habitats compared to shallow, highly lit environments, while the branch diameter does not change (Kaniewska et al. 2008). It has been shown that this variation in colony morphology allows corals to optimize light-dependent performance (Kaniewska et al. 2008). There is, however, a need to discern whether these morphologically variable colonies inhabiting different light regimes have different photosynthetic performances and thus fitness potential. We hypothesize that phenotypic plasticity in branching corals across light habitats should maximize potential light utilization and photosynthesis. The aim of this study was to determine whether this is true for the phenotypically plastic *A. humilis* across environmental irradiance levels. To determine this, we mapped differences in light levels at various locations within *A. humilis* colonies found at 5 and 18 m and estimate the correlation between observed within-colony light variation and photosynthetic capacity. It is expected that a heterogeneous light field will result in both photoacclimation state and maximum productivity heterogeneity across coral surfaces, both of which will have consequences for whole-colony photosynthetic capacity. In particular, we expect that in an *A. humilis* colony, the greatest difference in the light field and consequently the photobiology will be between inner and outer branches. This is because outer branches at the periphery extend at an angle rather than vertically like the central branches, which can cause differences in light fields experienced by two sides on an outer branch, while the light field should be more uniform on two sides in a central branch. In addition, we quantify whole-colony surface light distribution and photosynthetic capacity for *A. humilis*, and its different phenotypes at 5 and 18 m and explore which parameter is most influential in determining whole-colony photosynthetic capacity.

Materials and methods

Within-colony light measurements

To determine whole-colony light distribution for *A. humilis* phenotypes at 5 and 18 m, within-colony light profiles of a total of 10 colonies at each depth were conducted around midday (11:00–14:00) on cloudless days, to minimize potential variations due to changes in the ambient light regime. Colonies were chosen, which were growing on similar benthos to make sure that the light-scattering properties of the surrounding environment (reef rock with encrusting algae in this case) were similar between colonies. These measurements were taken at Tenements 1 (23°25.983'S, 151°55.756'E) Heron Reef, Capricorn Bunker group, Southern Great Barrier Reef. Twelve irradiance profiles were performed on each colony, and they

were conducted within a short time frame for each colony (<5 min per profile). In the absence of a logistically feasible system with which to measure scalar irradiance underwater in situ inside coral colonies, we measured point irradiance (PAR, photosynthetically active radiation) using a small cosine-corrected miniature fibre optics quantum sensor (Diving-F1, Walz, Germany) attached to a submersible fluorometer (Diving-Pam, Walz, Germany). The light sensor was calibrated against a factory calibrated Li-192 Li-Cor cosine-corrected underwater light sensor. Measurements of incident downwelling light were first read at the tip of the branch with the sensor held horizontally. Consecutive measurements were taken with increasing distance from the tip following the orientation of the polyps on the side of the branch. This way, the light profile would represent a “polyp view” of the incident light at various parts of the branch (Anthony et al. 2005). The reasoning for this approach was that ideally these measurements would be done using a scalar irradiance probe allowing light from all directions to be captured, which would be a true measure of the light field. However, in the absence of such measurements, a “polyp view” of point irradiance is more representative of the light field for the coral polyps at the surface of the coral branches, compared to measurements where the point irradiance is measured horizontally, which would not represent incident light experience by the coral surface at that point. Irradiance profiles for 10 colonies at each of 5 and 18 m were performed. Within-colony irradiance profiles were conducted from 3 compass directions (north, south-east and south-west). An outside branch and an inside branch were measured for each compass direction, adding up to 6 branches in total measured for each colony (Fig. 1). Twelve irradiance profiles were conducted on 6 branches for each colony, two irradiance profiles for each branch, one light profile on the outside facing side of the branch (side a) and one light profile on the inside facing side of the branch (side b) (Fig. 1). This meant that for side b of the outer branches, light measurements were taken with the probe carefully placed (held by the cable away from the colony as to prevent self-shading) facing the benthos as this was the polyp view for these coral surfaces. Incident downwelling irradiance at the branch tip with the sensor held horizontally provided an estimate of ambient light at the time of the measurement, and it was used as a reference point for the light profiles. Consecutive irradiance measurements within a light profile were converted to a percentage of the reference point in order to account for potential variations in the ambient light regimes.

Coral collection

In order to determine photosynthetic capacity of different coral surfaces within a branching coral colony, *A.*

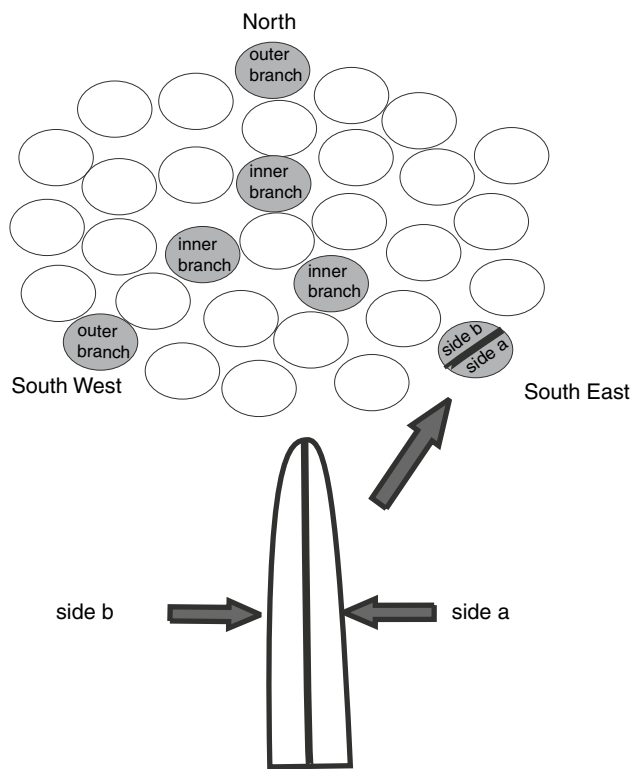


Fig. 1 Schematic illustration of branch surface locations within *Acropora humilis* colonies at 5 and 18 m used for determining light attenuation profiles and chlorophyll *a* fluorescence measurements. Branch surfaces used were from three compass directions (north, south-east and south-west) and two sides (*side a* and *side b*) of an inner and outer branch from each compass direction

humilis branches were sampled at Tenements 1 from the same colonies, which had been used for light measurements mentioned above. Six whole branches per colony were collected from 10 colonies at 5 m and 10 colonies at 18 m. The colony size was 25–35 cm in diameter for all colonies used in the study. Three branches from the outside of the colony from 3 compass directions north (N), south-east (SE) and south-west (SW) and 3 branches from the inner most part of the colony from 3 compass directions (Fig. 1) were collected. At the time of collection, branches were marked next to the cut surface at the base of the branch on the outside orientation of the branch so that this orientation could later be maintained in aquaria prior to further processing. Following collection, *A. humilis* branches were transported under shaded conditions ($<50 \mu\text{mol photons m}^{-2} \text{s}^{-1}$) through the use of shade cloths to through-flow aquaria at Heron Island Research Station. Here, they were kept in ambient temperatures under low-light conditions ($<50 \mu\text{mol photons m}^{-2} \text{s}^{-1}$), until chlorophyll *a* fluorescence measurements were taken after 60 min of dark acclimation at dusk, to ensure complete relaxation of the photosystems;

traditionally, this is thought to be at least 20 min of dark adaptation (Ralph and Gademann 2005).

Chlorophyll *a* fluorescence measurements

Photosynthetic capacity of different coral surfaces within an *A. humilis* coral colony was determined using chlorophyll *a* fluorescence and rapid light curves (RLC). After dark acclimation of coral branches, two-dimensional heterogeneities in photosynthetic capacity of endosymbiotic *Symbiodinium* were detected using the Maxi ($70 \times 100 \text{ mm}$ field) Imaging-PAM (Walz GmbH, Effeltrich, Germany). For each branch, both sides (a) and (b) were imaged (Fig. 1). Relative electron transport rate (rETR) was calculated as $\Phi_{\text{PSII}}' \times \text{EPAR}$, where Φ_{PSII}' (effective quantum yield) is $(F_m' - F)/F_m'$ (Hill et al. 2004), and EPAR is irradiance within the photosynthetically active range (PAR 400–700 nm); the majority of LEDs from the Maxi Imaging-PAM emit light at 460, but there is a proportion that also emits at 650 and 780 nm. Considering that red light attenuates more rapidly with depth underwater (Kirk 1994), light emitted at 460 nm will still apply to corals grown both at 5 and 18 m on Heron Island, as this is in the blue region of the spectrum. RLC were performed where measurements of rETR were obtained by applying a series of saturation pulses under LED-emitted increasing actinic irradiance (0, 4, 40, 60, 80, 100, 135, 175, 225, 290, 365, 460, 585, 746, 956 $\mu\text{mol photons m}^{-2} \text{s}^{-1}$) RLC (Ralph and Gademann 2005). At the end of each 20-s period, a saturation pulse was applied at each irradiance level to determine Φ_{PSII}' . Areas of interest were superimposed over the image using ImagingWin software (v1.00b, Walz GmbH). In order to obtain descriptive parameters of relative ETR_{max} (rETR_{max}, maximum relative electron transport rate), quantum efficiency of photosynthesis (Φ_{PSII}) and α (light limited initial slope of the RLC), methods in Silsbe and Kromkamp (2012) were followed and RLC of each area of interest were fitted to an E-normalized form of the hyperbolic tangent model (Jassby and Platt 1976), using STATISTICA 7.0 (StatSoft Inc). To obtain a more accurate value of E_k (light saturation coefficient), methods were followed from Henninge et al. (2008), and values of E_k were estimated by fitting RLC to Eq. (1) in Henninge et al. (2008), using STATISTICA 7.0 (StatSoft Inc).

Symbiodinium identification

The genotype of the resident *Symbiodinium* in *A. humilis* colonies used in this study was identified by denaturing gel electrophoresis (DGGE) of the internal transcriber spacer 2 (ITS2) region of nuclear ribosomal DNA (cf. LaJeunesse et al. 2003) and following the methods in (Sampayo et al.

Table 1 Nonlinear regression summary of different irradiance models for *Acropora humilis* at different locations within a colony at 5 and 18 m

| Irradiance model | 5 m | | | 18 m | | |
|---------------------|-------------------------------|--------------|-------|-------------------------------|--------------|-------|
| | $E_{(d)} = E_{(o)} \exp(-bd)$ | | | $E_{(d)} = E_{(o)} \exp(-bd)$ | | |
| Branch location | $I_{(o)}$ | b | r^2 | $I_{(o)}$ | b | r^2 |
| North | | | | | | |
| Inner branch side a | 0.99 ± 0.022 | 0.93 ± 0.047 | 0.94 | 1.00 ± 0.021 | 0.66 ± 0.029 | 0.94 |
| Inner branch side b | 0.98 ± 0.027 | 0.95 ± 0.061 | 0.91 | 0.99 ± 0.028 | 0.59 ± 0.035 | 0.89 |
| Outer branch side a | 0.98 ± 0.023 | 1.43 ± 0.090 | 0.91 | 0.99 ± 0.018 | 1.50 ± 0.077 | 0.96 |
| Outer branch side b | 1.02 ± 0.040 | 0.58 ± 0.047 | 0.83 | 1.00 ± 0.040 | 0.52 ± 0.043 | 0.79 |
| South-east | | | | | | |
| Inner branch side a | 0.99 ± 0.024 | 0.92 ± 0.047 | 0.93 | 0.99 ± 0.024 | 0.63 ± 0.035 | 0.91 |
| Inner branch side b | 1.00 ± 0.020 | 0.93 ± 0.043 | 0.94 | 1.00 ± 0.018 | 0.64 ± 0.025 | 0.96 |
| Outer branch side a | 0.99 ± 0.028 | 1.50 ± 0.121 | 0.88 | 0.99 ± 0.023 | 1.30 ± 0.078 | 0.93 |
| Outer branch side b | 1.01 ± 0.050 | 0.55 ± 0.055 | 0.73 | 1.02 ± 0.033 | 0.50 ± 0.032 | 0.85 |
| South-west | | | | | | |
| Inner branch side a | 0.99 ± 0.014 | 0.93 ± 0.032 | 0.97 | 1.00 ± 0.017 | 0.75 ± 0.028 | 0.96 |
| Inner branch side b | 0.99 ± 0.025 | 0.92 ± 0.039 | 0.95 | 1.00 ± 0.028 | 0.63 ± 0.038 | 0.91 |
| Outer branch side a | 0.99 ± 0.024 | 1.31 ± 0.083 | 0.92 | 0.99 ± 0.021 | 1.20 ± 0.062 | 0.95 |
| Outer branch side b | 1.02 ± 0.040 | 0.62 ± 0.049 | 0.83 | 1.02 ± 0.038 | 0.60 ± 0.046 | 0.84 |

Estimated coefficients are presented with ± standard error, where $I_{(d)}$ is irradiance at position d along the branch, I is a maximum irradiance coefficient, and b is a light attenuation coefficient

2009). Briefly, ITS2 was amplified using primer sequences of LaJeunesse et al. (2003). Profiles were compared with symbiont profiles generated by Sampayo et al. (2007, 2008, 2009). Prominent DGGE bands were excised, sequenced and identified as described in Sampayo et al. (2009). *Symbiodinium* identity was determined for 5 colonies of *A. humilis* at 5 m and 5 colonies of *A. humilis* at 18 m. In addition, DNA extractions were done on 6 branches from each colony from the 3 compass directions (Fig. 1), and the symbiont genotypes were determined from top and base parts of branches.

Data analysis

All data were tested for normality and homogeneity of variance, and where assumptions were violated, the data were corrected by transformations. Nonparametric equivalent tests were used when data did not meet the assumptions of normality and homogeneity of variance, or could not be normalized using transformations.

In the absence of a formal theory for light attenuation within branching coral colonies, linear and exponential best fits to the light profile data within colonies were used. We found that nonlinear regressions provided the best fit and were therefore used to determine the rate of within-colony light attenuation. A factorial analysis of variance (ANOVA) was used to test the effects of depth, compass direction, branch position and branch surface on $rETR_{max}$, E_k and α . All analyses were performed using STATISTICA 7.0 (Stat-Soft Inc).

Whole-colony light distribution

Based on the light attenuation profiles derived from nonlinear regression described above (Table 1), whole-colony branch light distribution was simulated using the maximum daily irradiance values recorded at a given habitat, according to methods described in (Kaniewska et al. 2008; Kaniewska et al. 2011), which at 5 m was $577 \pm 107 \mu\text{mol photons m}^{-2} \text{ s}^{-1}$ and in the deep it was $116 \pm 22 \mu\text{mol photons m}^{-2} \text{ s}^{-1}$. Nonlinear regressions for light attenuation profiles were forced through the origin, as this light value represented light experienced by the axial tip of the branch and would be used to correspond to chlorophyll *a* fluorescence measurements at the tip. Light attenuation models from all areas within a colony were used to create a frequency distribution of light experienced by the entire colony. A *t* test of light distribution Kurtosis was used to determine differences in whole-colony light distribution for *A. humilis* phenotypes at 5 and 18 m.

Whole-colony rETR

Based on the chlorophyll *a* fluorescence measurements along branches at different positions in the colony, whole-colony distributions of $rETR_{max}$ and E_k were simulated by incorporating light (nonlinear regression coefficients from light attenuation profiles, Table 1) and chlorophyll *a* fluorescence data (mean and SE from parameter estimates of $rETR_{max}$ and E_k , Table 2, and $rETR_{max}$ and E_k values for the tip of a branch correspond to incident light at the tip of

Table 2 Summary statistics of rapid light curve parameters $rETR_{max}$, E_k and α for different surface areas within *Acropora humilis* colonies at 5 and 18 m

| Geographical direction | Branch position | 5 m | | | | | | 15 m | | | | | | | | | | | | |
|------------------------|-----------------|----------------|-------|--------------|-------|-------|-------|----------|-------|-------|-------|--------------|-------|-------|-------|----------|----|------|----|--|
| | | Branch surface | | $rETR_{max}$ | | E_k | | α | | N | | $rETR_{max}$ | | E_k | | α | | N | | |
| | | Mean | SE | Mean | SE | Mean | SE | Mean | SE | Mean | SE | Mean | SE | Mean | SE | Mean | SE | Mean | SE | |
| North | Inner | Top side a | 115.5 | 4.23 | 187.5 | 8.28 | 0.616 | 0.008 | 10 | 119.7 | 3.48 | 185.4 | 7.16 | 0.646 | 0.011 | 10 | | | | |
| | | Base side a | 90.9 | 6.36 | 138.7 | 12.17 | 0.656 | 0.017 | 10 | 94.2 | 3.83 | 146.5 | 7.09 | 0.643 | 0.016 | 10 | | | | |
| | Outer | Top side b | 122.7 | 4.64 | 200.2 | 7.96 | 0.613 | 0.007 | 10 | 126.6 | 2.55 | 197.3 | 5.07 | 0.642 | 0.011 | 10 | | | | |
| | | Base side b | 94.8 | 6.51 | 147.7 | 9.60 | 0.642 | 0.006 | 10 | 106.6 | 4.97 | 166.0 | 9.36 | 0.642 | 0.011 | 10 | | | | |
| | | Top side a | 97.3 | 4.01 | 158.1 | 6.51 | 0.616 | 0.005 | 10 | 106.5 | 6.75 | 163.9 | 10.23 | 0.650 | 0.011 | 10 | | | | |
| | | Base side a | 73.6 | 7.14 | 112.3 | 12.15 | 0.656 | 0.033 | 10 | 67.4 | 7.08 | 106.8 | 9.92 | 0.631 | 0.019 | 10 | | | | |
| South-east | Inner | Top side b | 117.4 | 4.85 | 186.4 | 9.12 | 0.630 | 0.008 | 10 | 118.0 | 7.03 | 187.4 | 10.07 | 0.630 | 0.010 | 10 | | | | |
| | | Base side b | 78.5 | 6.47 | 122.5 | 10.62 | 0.641 | 0.012 | 10 | 96.0 | 8.81 | 151.5 | 13.49 | 0.634 | 0.012 | 10 | | | | |
| | Outer | Top side a | 118.2 | 5.14 | 190.6 | 8.31 | 0.620 | 0.009 | 9 | 121.9 | 2.83 | 190.0 | 4.67 | 0.641 | 0.007 | 10 | | | | |
| | | Base side a | 80.7 | 6.28 | 126.6 | 9.57 | 0.637 | 0.005 | 9 | 96.9 | 4.87 | 150.2 | 8.85 | 0.645 | 0.016 | 10 | | | | |
| | | Top side b | 120.8 | 4.75 | 196.1 | 9.80 | 0.616 | 0.006 | 10 | 122.1 | 4.93 | 185.6 | 8.67 | 0.658 | 0.012 | 10 | | | | |
| | | Base side b | 93.5 | 5.89 | 147.5 | 7.52 | 0.634 | 0.013 | 10 | 91.7 | 6.10 | 141.1 | 9.95 | 0.650 | 0.009 | 10 | | | | |
| South-west | Inner | Top side a | 95.0 | 5.56 | 154.5 | 10.39 | 0.615 | 0.016 | 10 | 101.0 | 6.19 | 160.5 | 11.17 | 0.630 | 0.006 | 10 | | | | |
| | | Base side a | 64.7 | 5.18 | 112.0 | 9.73 | 0.577 | 0.011 | 10 | 75.9 | 6.97 | 126.6 | 12.58 | 0.599 | 0.014 | 10 | | | | |
| | Outer | Top side b | 116.3 | 6.37 | 185.4 | 9.97 | 0.627 | 0.007 | 10 | 113.2 | 5.79 | 176.0 | 8.03 | 0.643 | 0.013 | 10 | | | | |
| | | Base side b | 99.4 | 7.06 | 155.3 | 11.51 | 0.640 | 0.009 | 10 | 88.4 | 7.39 | 136.0 | 11.56 | 0.650 | 0.010 | 10 | | | | |
| | | Top side a | 107.0 | 10.03 | 171.2 | 16.48 | 0.625 | 0.008 | 10 | 119.3 | 2.98 | 181.6 | 5.65 | 0.657 | 0.009 | 10 | | | | |
| | | Base side a | 81.8 | 7.84 | 124.0 | 11.82 | 0.660 | 0.010 | 10 | 82.8 | 4.26 | 126.4 | 7.41 | 0.655 | 0.009 | 10 | | | | |
| Outer | Top side b | 124.8 | 3.71 | 203.6 | 6.84 | 0.613 | 0.010 | 10 | 121.4 | 3.85 | 185.0 | 7.66 | 0.656 | 0.011 | 10 | | | | | |
| | Base side b | 104.5 | 4.63 | 167.0 | 8.00 | 0.626 | 0.009 | 10 | 98.1 | 5.08 | 150.8 | 8.31 | 0.651 | 0.010 | 10 | | | | | |
| | Top side a | 98.4 | 6.23 | 154.3 | 11.17 | 0.637 | 0.010 | 10 | 98.0 | 6.05 | 149.9 | 10.01 | 0.654 | 0.011 | 10 | | | | | |
| | Base side a | 71.2 | 7.87 | 112.5 | 13.58 | 0.633 | 0.011 | 10 | 80.7 | 8.41 | 126.8 | 14.39 | 0.637 | 0.011 | 10 | | | | | |
| Outer | Top side b | 122.1 | 5.05 | 197.2 | 9.80 | 0.619 | 0.011 | 10 | 116.1 | 3.80 | 182.7 | 6.49 | 0.635 | 0.011 | 10 | | | | | |
| | Base side b | 93.2 | 8.80 | 144.4 | 14.03 | 0.646 | 0.009 | 10 | 98.2 | 3.62 | 154.6 | 6.06 | 0.635 | 0.009 | 10 | | | | | |

The mean top area of a branch represents the first 2 cm away from the branch tip, and the mean base area of a branch represents the first 2 cm away from the branch base
SE standard error of the mean

a branch) from different locations within a colony. To calculate a rETR for a whole colony, the hyperbolic tangent model was used (Jassby and Platt 1976) (Eq. 1) using simulated values for $rETR_{\max}$ and E_k described above together with simulated whole-colony irradiance estimates at various positions in the colony (E) derived above.

$$rETR = rETR_{\max} \tanh\left(\frac{E}{E_k}\right) \quad (1)$$

Kruskal–Wallis tests for rETR distribution Kurtosis were used to determine differences in rETR distribution among positions within an *A. humilis* colony and between depths. Two-way ANOVA was used to determine difference in rETR and Φ_{PSII} distribution as a function of ambient light levels (at 5 or 18 m) and type morphology model (type morphology for colonies at 5 or 18 m).

Sensitivity analysis

To evaluate which parameters (depth, geographical position, branch position or branch side) are the most influential in estimating whole-colony rETR at each depth, sensitivity analysis was done. This was done through a local sensitivity analysis (Hamby 1994) where one parameter at a time was varied while the others were fixed; these parameters were increased and decreased by 1–3 standard deviations, and associated output values were calculated using Excel and PopTools (ver. 3.2.5) (Hood 2010). The sensitivity index (SI) was calculated using Eq. (2)

$$SI = \frac{D_{\max} - D_{\min}}{D_{\max}}, \quad (2)$$

where D_{\min} and D_{\max} are the minimum and maximum output values, resulting from varying the input as described above (Hamby 1994). In addition, a rank regression coefficient (RRC) was calculated by performing regression analysis on rank-transformed input versus output values from the sensitivity analysis (Hamby 1994). Higher values of both the SI and RCC indicate that a parameter is more influential in determining the model output, which in this case is the estimation of whole-colony rETR.

Results

Within-colony light profiles

Based on the field light data, irradiance profiles varied among different positions within the colonies (Table 1). The greatest light attenuation, based on the nonlinear regression coefficients (Table 1) at both depths, was found on side (a) (definition, Fig. 1) in outer branches, where on average across the three compass directions,

44 % more light was attenuated compared to inner branches in the shallow colonies and 93 % more light was attenuated compared to inner branches in the deep colonies. Conversely, the least steep attenuation coefficient b (Table 1) at both depths was found on side (b) (definition, Fig. 1) of the outer branches, where the difference was a 59, 64 and 53 % decrease in light attenuation compared to side (a) of outside branches in the shallow and a 65, 62 and 50 % decrease in light attenuation compared to side (a) of outside branches in the deep for N, SE and SW compass directions, respectively. There were differences in light attenuation for inside branches between the two depths where the light attenuation coefficient b (Table 1) was 50, 45 and 35 % greater in the shallow compared to the deep for N, SE and SW compass directions, respectively.

Symbiodinium identification

Acropora humilis colonies from both 5 and 18 m harboured the same *Symbiodinium* symbionts. There were also no within-colony differences detected in *Symbiodinium* genotypes for all colonies. By sequence identity, the symbionts were found to be C1 when compared to known *Symbiodinium* ITS2 sequences on GenBank (www.ncbi.nih.gov).

Chlorophyll *a* fluorescence

Photosynthetic activity of *Symbiodinium*, indicated by parameters $rETR_{\max}$, E_k and α , varied among different coral surfaces within colonies, where there were differences between inner and outer branches, as well as between side a and b of branch, top and base (Table 3). Depth and compass direction only affected α (Table 3). The greatest difference along the branch was between the top part of side (b) and base part side (a) of an outer branch, where there was a 46 % increase in $rETR_{\max}$, 52 % increase in E_k and a 3 % decrease in α . This reflects the light attenuation trends within coral colonies described above and therefore potential light environment for the coral tissues at these locations, as at both depths, coral surfaces for outer branches side a had the least light while upper surfaces of outer branches side b had the most light, based on the steepest and least steep attenuation coefficients b described above (Table 1). At both depths, inner branches had greater photosynthetic potential compared to outside branches, with an overall 11 % increase in $rETR_{\max}$ and 12 % increase in E_k . Branches from the SW compass direction had the highest α , 2 % higher than the other two directions. Coral surfaces from colonies found in the deep had a 2 % increase in α compared to coral surfaces from colonies in the shallow (Table 2).

Table 3 Summary of factorial ANOVA results for *Acropora humilis* rapid light curve parameters; $rETR_{max}$, E_k and α , with depth (5 and 18 m), geographical compass directions (north, south-east and south-

west), branch position (inner or outer) and branch surface (side a and side b, top and base) as sources of variance

| Source of variance | $rETR_{max}$ | | | E_k | | | α | | |
|---|--------------|-------|------------------|-------|-------|------------------|----------|------|------------------|
| | df | F | p | df | F | p | df | F | p |
| Depth | 1 | 3.70 | ns | 1 | 0.23 | ns | 1 | 15.2 | <0.001 |
| Geographical direction | 2 | 0.12 | ns | 2 | 0.14 | ns | 2 | 2.8 | ns |
| Branch position | 1 | 43.00 | <0.001 | 1 | 32.22 | <0.001 | 1 | 4.7 | 0.030 |
| Branch surface | 3 | 99.62 | <0.001 | 3 | 94.83 | <0.001 | 3 | 1.3 | ns |
| Depth x geographical direction | 2 | 0.59 | ns | 2 | 0.82 | ns | 2 | 1.2 | ns |
| Depth x branch position | 1 | 0.00 | ns | 1 | 0.11 | ns | 1 | 2.7 | ns |
| Geographical direction x branch position | 2 | 1.34 | ns | 2 | 1.43 | ns | 2 | 1.3 | ns |
| Depth x branch surface | 3 | 1.31 | ns | 3 | 1.84 | ns | 3 | 3.7 | 0.012 |
| Geographical direction x branch surface | 6 | 0.44 | ns | 6 | 1.04 | ns | 6 | 3.1 | 0.006 |
| Branch position x branch surface | 3 | 2.72 | 0.044 | 3 | 2.45 | ns | 3 | 3.7 | 0.012 |
| Depth x geographical direction x branch position | 2 | 0.10 | ns | 2 | 0.28 | ns | 2 | 0.2 | ns |
| Depth x geographical direction x branch surface | 6 | 1.58 | ns | 6 | 1.43 | ns | 6 | 0.7 | ns |
| Depth x branch position x branch surface | 3 | 0.16 | ns | 3 | 0.18 | ns | 3 | 0.9 | ns |
| Geographical direction x branch position x branch surface | 6 | 0.72 | ns | 6 | 0.68 | ns | 6 | 1.1 | ns |
| Depth x geographical direction x branch position x branch surface | 6 | 0.54 | ns | 6 | 0.53 | ns | 6 | 0.3 | ns |
| Total | 430 | | | 430 | | | 421 | | |

Significant results are highlighted in bold

Light distribution across colonies

In order to estimate the light field across a whole colony at the two depths, light attenuation profiles derived from nonlinear regression on field light data (Table 1) described above were applied to model light distributions across the surface of whole colonies, and in this study, this included branches from the periphery. Our modelled light distributions showed that *A. humilis* colonies at both depths had a similar PAR mode of the colony light distributions, despite differences in ambient light input being fivefold (Fig. 2). At both depths, the modal irradiance was $50 \mu\text{mol m}^{-2} \text{s}^{-1}$. The shallow colony light distribution had a greater range in light levels above $200 \mu\text{mol m}^{-2} \text{s}^{-1}$. To confirm the differences in frequency distribution of modelled whole-colony light distributions between coral colonies at the two depths, Kurtosis analysis of both light distributions was done and revealed these differences (t test, $t_5 = 34.1$, $p < 0.001$) (Fig. 2).

Whole-colony photosynthetic activity

In order to estimate whole-colony rETR distributions, we applied chlorophyll *a* fluorescence data (E_k and $rETR_{max}$) for different positions within a coral colony at both depths together with modelled whole-colony PAR distributions described above and fitted this data to Eq. (1). This modelled frequency distribution of rETR for different colony

positions showed similarities among compass directions and between depths, where side (a) of outer branches had the highest modal rETR distribution in the lowest rETR category, $10 \mu\text{mol e}^- \text{m}^{-2} \text{s}^{-1}$ (Fig. 3). The deep side (b) of outer branches and side (a) and (b) of inner branches had similar rETR distributions, while the shallow side (b) of outer branches had a higher rETR mode compared to side (a) and (b) of inner branches (Fig 3). We did Kurtosis analysis on the frequency distribution of modelled whole-colony rETR distributions to confirm differences in these depending on branch position (inner vs. outer) (Kruskal–Wallis test, $H_{1,120} = 4.15$, $p = 0.042$) and branch side (side a vs. side b) (Kruskal–Wallis test, $H_{1,120} = 36.62$, $p < 0.001$) (Fig. 3). In order to determine whether the colony morphology present at the two depths represented an optimal morphology for potential energy utilization of the whole-colony, we applied the ambient light levels found at 5 and 18 m to both deep and shallow models for estimating whole-colony rETR. Estimates of whole-colony rETR capacity varied with ambient light levels (two-way ANOVA, $F_{1,16} = 268,443$, $p < 0.001$) among type morphology models (deep and shallow) (two-way ANOVA, $F_{1,16} = 19,295$, $p < 0.001$) and as a function of both ambient light level and type morphology model (two-way ANOVA, $F_{1,16} = 5,167$, $p < 0.001$). In shallow colonies at ambient light levels in the shallow, estimated whole-colony rETR was twice that found in deep colonies at ambient light levels in the deep. Comparing the whole-colony rETR at deep

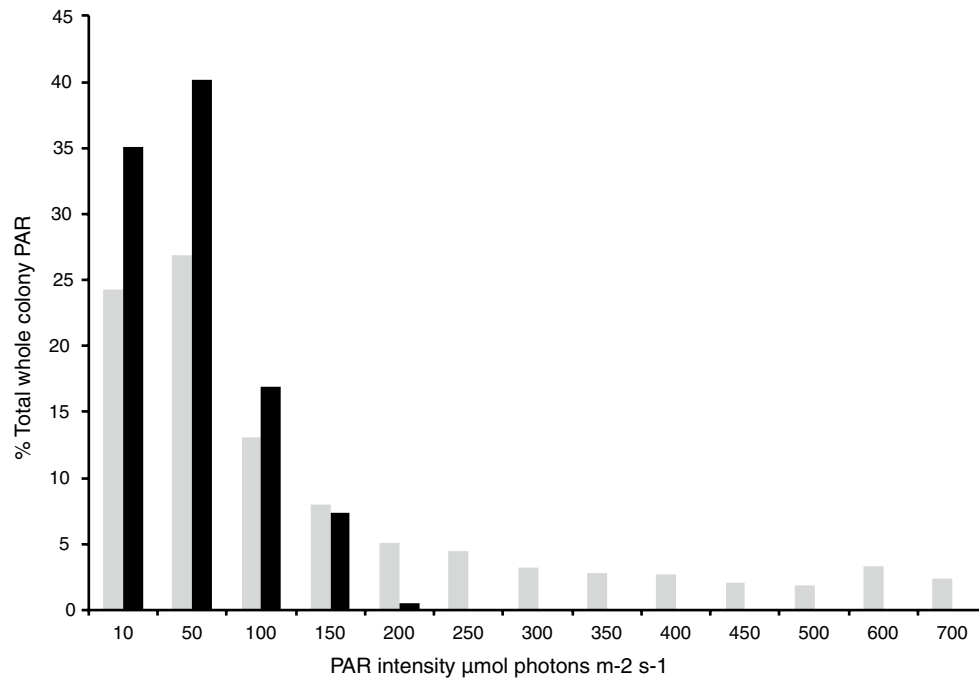


Fig. 2 Whole-colony PAR distribution for external surface irradiance in *Acropora humilis* at 5 m (grey) and 18 m (black) at Heron Island. The light distributions were obtained from 100 Monte Carlo iterations using the mean daily maximum irradiance as input value and esti-

imated best-fit function parameters for tissue surface light attenuation profile coefficients. The light distributions are given as percentages across irradiance categories of the total whole-colony PAR level

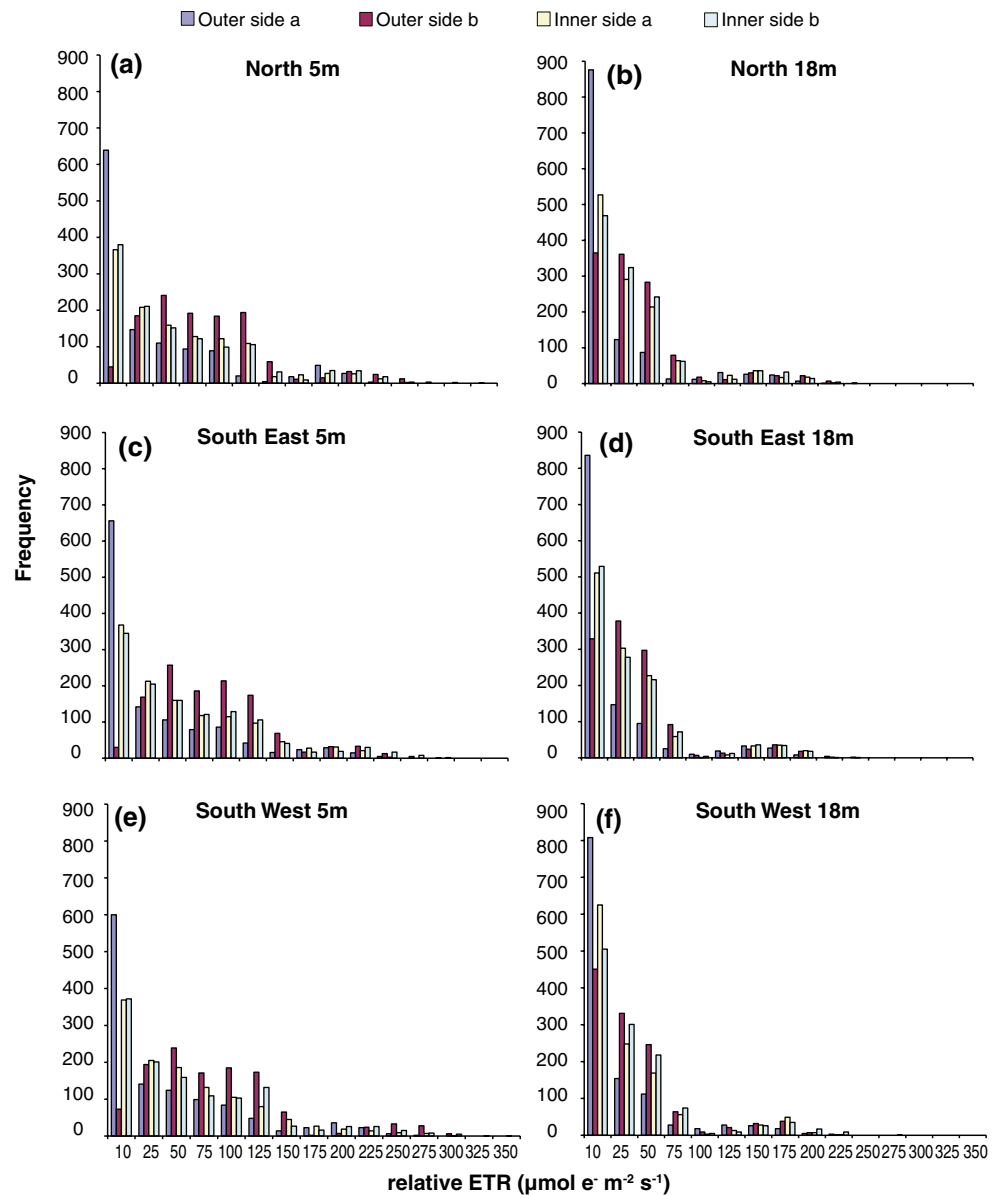
ambient light levels for deep and shallow type morphology models revealed that the deep type morphology increased rETR capacity by 17 %. At shallow ambient light levels, the deep type morphology increased rETR capacity by 25 % (Table 4). We also report here modelled whole-colony Φ_{PSII} values to demonstrate that the same trends as in the whole-colony rETR modelling data are present (Table 4) (Supplementary Fig. 1), as it has been suggested that modelling the E-dependency of Φ_{PSII} results in more precise and accurate photosynthesis-irradiance data when derived from chlorophyll *a* fluorescence measurements (Silsbe and Kromkamp 2012). Here, we found that estimates of whole-colony Φ_{PSII} values mimicked the whole-colony rETR data, although reverse in magnitude since it is the inverse relationship with *E* as compared to rETR versus *E*. Φ_{PSII} varied with ambient light levels (two-way ANOVA, $F_{1,16} = 186$, $p < 0.001$), among type morphology models (deep and shallow) (two-way ANOVA, $F_{1,16} = 35,661$, $p < 0.001$) and as a function of both ambient light level and type morphology (two-way ANOVA, $F_{1,16} = 228$, $p < 0.001$) (Table 4).

Sensitivity analysis

To determine which parameters are most influential in estimating the whole-colony rETR (depth, geographical position, branch position or branch side), sensitivity

analysis of model parameters was performed. Assessment of the influence of each parameter is indicated by the SI and the RCC (Table 5). The highest differences in both SI and RCC were observed for branch position (inner vs. outer), indicating that branch position is the most influential parameter in the model estimating whole-colony photosynthetic activity. The second most influential parameter was branch side (a vs. b), while geographical direction had the smallest influence on whole-colony photosynthetic activity. Combined parameters branch position \times branch side show that the outer branch side (a) is the least influential in determining whole-colony photosynthetic activity compared to inner sides (a) and (b), and this stays true even when separated into the three geographical directions (Table 5). These trends were the same for both deep and shallow colonies, and there were only minor differences in SI and RCC between parameters across the two depths (Table 5). In order to investigate the relative role of photochemical versus non-photochemical quenching in driving the variance observed in E_k (Tables 2, 3), values for photochemical quenching (qP) and non-photochemical quenching (NPQ) were plotted against E/E_k (Fig. 4). The light response curves of qP were constant between different positions within coral colonies, and this was the same across the two depths (Fig. 4a, b), where qP decreased with increasing light. In contrast, trends in NPQ in response

Fig. 3 Estimated whole-branch relative electron transport rate (rETR) distribution for *Acropora humilis* at 5 m (a, c and e) and 18 m (b, d and f), from compass directions north (a, b) south-east (c, d) and south-west (e, f). Each distribution was obtained from 100 Monte Carlo iterations using Eq. (1), where E is the whole-colony irradiance distributions (Fig. 2) and $rETR_{max}$ and E_k are estimated from rapid light curve measurements (Table 2)



to increasing light showed an increase in NPQ. For both depths, the lowest curve was observed for outer side a branches, and this difference was amplified in shallow colonies where the NPQ curves for the inner branches side a and b were greater (Fig. 4c, d). Changes in F_0 (minimum fluorescence yield—dark-adapted) versus E/E_k were also plotted to investigate how this potential proxy for pigmentation changes across colony positions at the two depths. There was only a trend in the shallow colonies where the outer side a had higher F_0 values compared to the other coral surfaces within shallow corals (Fig. 4e, f). These differences in trends for NPQ and F_0 highlight results from the sensitivity analysis, which showed that branch position was the most influential parameter in estimating whole-colony rETR.

Discussion

The irradiance profiles of *A. humilis* varied within colonies depending on branch location and branch side. These differences were similar to changes in three orders of magnitude in light differences reported within sea grass canopies (Enriquez et al. 2002). Differences were the greatest between sides (a) and (b) of outer branches but not for the (a) and (b) sides of inner branches. At both depths, the darkest part of an *A. humilis* colony is on the outer side of a branch at the periphery (side a) where light is attenuated the most, which is primarily due to the fact that these branches extend at an angle rather than vertically like the central branches. Conversely, the inner or upward side of peripheral branches (side b) would be expected to be

Table 4 Summary statistics of whole-colony relative electron transport rate (rETR) and the E-dependency of quantum efficiency of photosynthesis (Φ_{PSII}) estimates at ambient light conditions at 5 and 18 m, and for two type morphologies shallow model (5 m) and deep model (18 m)

| | Mean whole-colony rETR \pm SE ($\mu\text{mol e}^- \text{m}^{-2} \text{s}^{-1}$) | Mean whole-colony $\Phi_{PSII} \pm$ SE |
|-----------------------|---|---|
| Ambient light at 18 m | | |
| Shallow model | 27,935.8 \pm 40.4 | 862.1 \pm 0.78 |
| Deep model | 32,666.9 \pm 47.5 | 859.3 \pm 0.49 |
| Ambient light at 5 m | | |
| Shallow model | 64,079.5 \pm 96.4 | 685.1 \pm 0.88 |
| Deep model | 80,121.3 \pm 137.9 | 656.3 \pm 1.25 |

SE represents the standard error of the mean

sun-exposed, and the lowest attenuation at both depths was found on the inner surface (side b) of the outermost branches. Branches found in the central part of the colony extend vertically and are expected to show no differences between sides of branches, as was confirmed by the light attenuation profiles. Differences in within-colony light distribution between depths were apparent in the inner branches, which comprises the majority of branches in a colony, where shallow colonies had 50 % steeper light attenuation coefficients. This strategy for increasing self-shading through colony morphological variation might be seen as advantageous in a surrounding light environment, which is five times greater than that found in the deep (Kaniewska et al. 2008), to reduce the risk of photoinhibition and photodamage, and it could reduce the overall cost of colony investment into photoprotective mechanisms by reducing the proportion of coral surfaces exposed to supraoptimal irradiances levels (Anthony et al. 2005).

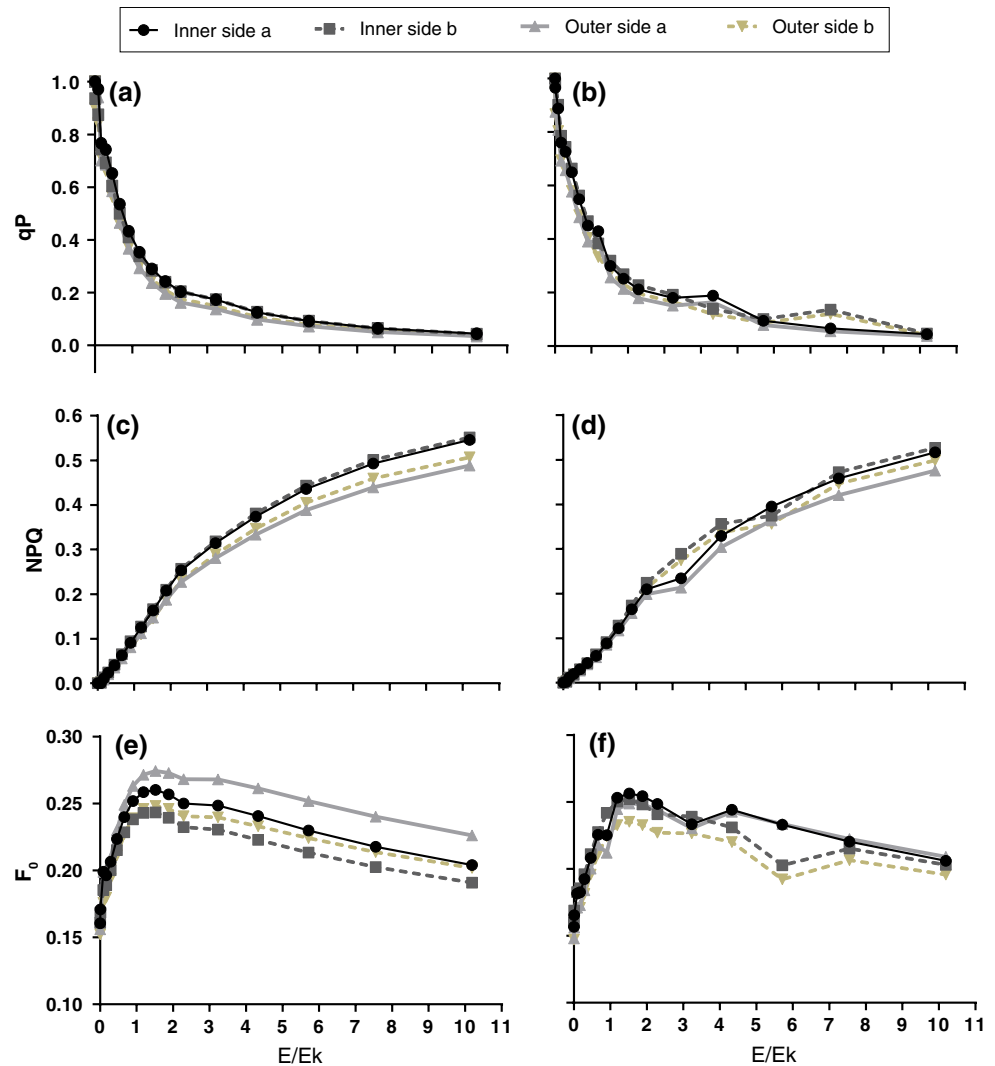
At both 5 and 18 m, the overall PAR light distributions incident on whole-colony surfaces were low, with the modal light range at both depths being around 50 $\mu\text{mol photons m}^{-2} \text{s}^{-1}$. Theoretically predicted optimal light levels within coral colonies should be light levels experienced by the photosynthetic units (i.e. *Symbiodinium* cells) such that light harvesting equals the turnover rate of the photosystems (Anthony and Hoegh-Guldberg 2003b). Anthony et al. (2005) estimated the optimal irradiance range to be 150–370 $\mu\text{mol photons m}^{-2} \text{s}^{-1}$ (based on the irradiance required to saturate photosynthesis, E_k) by examining photosynthesis-irradiance curves of *Symbiodinium*. A modal whole-colony light intensity distribution of 50 $\mu\text{mol photons m}^{-2} \text{s}^{-1}$, as found in this study, has been suggested to represent a suboptimal internal light environment. On the other hand, it has been shown that the within-colony surface irradiance measured does not accurately reflect the internal light environment reaching the photosynthetic symbiotic dinoflagellates (Kaniewska et al. 2011;

Table 5 Parameter sensitivity determination by the sensitivity index (SI) and the rank regression coefficient (RCC) of input versus output values in the sensitivity analysis of whole-colony rETR estimation

| | 18 m | | 5 m | |
|--|----------|------|----------|------|
| | SI index | RCC | SI index | RCC |
| Geographical direction | | | | |
| North | 0.417 | 28.6 | 0.400 | 28.8 |
| South-east | 0.401 | 28.1 | 0.403 | 28.1 |
| South-west | 0.387 | 27.8 | 0.393 | 28.0 |
| Branch position | | | | |
| Outer | 0.347 | 26.9 | 0.385 | 27.7 |
| Inner | 0.702 | 33.0 | 0.680 | 33.0 |
| Branch side | | | | |
| Side a | 0.522 | 30.8 | 0.498 | 30.5 |
| Side b | 0.585 | 32.1 | 0.599 | 32.1 |
| Branch position x branch side | | | | |
| Outer side a | 0.143 | 16.9 | 0.122 | 15.3 |
| Outer side b | 0.235 | 22.8 | 0.282 | 24.7 |
| Inner side a | 0.416 | 28.8 | 0.403 | 28.3 |
| Inner side b | 0.434 | 29.8 | 0.424 | 29.2 |
| Geographical direction x branch position x branch side | | | | |
| North outer side a | 0.049 | 8.0 | 0.049 | 7.9 |
| North outer side b | 0.088 | 13.1 | 0.102 | 14.0 |
| North inner side a | 0.164 | 18.8 | 0.157 | 18.9 |
| North inner side b | 0.172 | 21.0 | 0.158 | 19.3 |
| South-east outer side a | 0.050 | 8.5 | 0.046 | 7.4 |
| South-east outer side b | 0.088 | 13.5 | 0.101 | 13.3 |
| South-east inner side a | 0.168 | 19.9 | 0.147 | 17.3 |
| South-east inner side b | 0.166 | 19.3 | 0.168 | 20.4 |
| South-west outer side a | 0.052 | 9.0 | 0.053 | 8.8 |
| South-west outer side b | 0.079 | 12.1 | 0.104 | 14.4 |
| South-west inner side a | 0.152 | 17.8 | 0.154 | 18.4 |
| South-west inner side b | 0.170 | 20.4 | 0.160 | 19.9 |

Wangpraseurt et al. 2012) and that these light levels can be much lower (Kaniewska et al. 2011), but this depends on how deep within the tissues the algae resides as the light environment is largely heterogeneous within coral tissues (Wangpraseurt et al. 2012). This warrants a redefinition of optimal light levels actually reaching the photosynthetic unit in *Symbiodinium* as opposed to coral surface irradiance levels. There are many other photoacclimatory mechanisms present playing an important role in determining the actual light levels reaching the photosynthetic unit. *Symbiodinium* photosynthetic pigment concentrations can fluctuate to maximize light harvesting (Dubinsky et al. 1984; Falkowski and Dubinsky 1981; Porter et al. 1984). Reflective skeletal properties (Enriquez and Pantoja-Reyes 2005; Stambler and Dubinsky 2005) and, within coral tissue, multiple scattering and diffuse reflection can result in within-tissue light climates being higher than expected compared to incident

Fig. 4 Light response of **a**, **b** photochemical quenching (qP), **c**, **d** non-photochemical quenching (NPQ) and **e**, **f** F_0 (minimum fluorescence yield—dark-adapted) at 5 and 18 m. Each light response represents the mean of 10 rapid light curves from 10 colonies averaged across geographical compass direction for each colony. Standard error of the mean bars have been omitted for clarity. Light (E , $\mu\text{mol photons m}^{-2} \text{s}^{-1}$) is plotted relative to E_k



irradiance (Kuhl et al. 1995). To predict what optimal irradiances *Symbiodinium* requires, there is a need to measure actual light levels reaching the symbiotic dinoflagellate *in symbio*, which is not a straightforward task.

There was considerable variation in the photosynthetic efficiency of *Symbiodinium*, indicating differences in photoacclimation of the C1 symbiont, as the genotypes were the same across colonies and depths. Coral surfaces adapted to low-light conditions found on the outer surface (side a) of the outermost branches, and the coral surfaces at the base of innermost branches of the colony had lower values of $rETR_{\text{max}}$ and E_k compared to the inner surface of the outermost branches (side b) and top surfaces of the innermost branches in the colony, which are adapted to relatively high-light conditions. Changes in α showed a reverse trend, where high-light surfaces had lower values of α compared to low-light surfaces in the colony. This within-colony variability in photosynthetic capacity is consistent with variation in light levels. Previous studies have

also shown differences in photosynthetic capacity as a function of light intercepting the coral surface, where there are differences between upper and lower parts of the colony (Jones et al. 1998; Ralph et al. 2005) and differences along the upper part of a branch (Hill et al. 2004). Surfaces that have higher $rETR_{\text{max}}$, E_k and a less steep α can maintain a higher level of photosynthetic activity (Ralph and Gademann 2005). This is expected from coral surfaces adapted to high-light regimes, as there is potential for more photosynthesis with higher irradiance levels present, given that photoinhibition can be avoided through non-photochemical quenching pathways (Hoegh-Guldberg and Jones 1999; Jones et al. 1998). Depth only had a significant effect on α . Low-light-adapted coral surfaces, which have a higher α , can be photosynthetically more efficient at low irradiance levels compared to coral surfaces adapted to high-light levels (Chalker et al. 1983). It is important to note that with depth, there are changes not only in light quantity but also in light quality where a shift to the blue region

of the spectrum occurs with depth, and it has been shown that coral can be adapted chromatically to their surrounding light environment (Mass et al. 2010). It is not possible to directly relate chlorophyll *a* fluorescence to productivity as there is a nonlinear relationship between variable fluorescence and gross photosynthesis rate/oxygen concentration at high irradiances (Hoogenboom et al. 2006; Ulstrup et al. 2006). However, chlorophyll *a* fluorescence and RLC provide a useful assay for comparing relative light utilization and acclimation of photosystem II (Ralph and Gademann 2005). In addition, it has been recently discussed that caution is needed when determining energy utilization and budgets in scleractinian corals. Ideally, such a task requires, in addition to measures of photosynthesis and respiration, estimates of the biochemical composition of all constituents of energy currency in the cell (proteins, carbohydrates and lipids), an undertaking that has to date been a rare occurrence as almost all energetic approaches used in the coral literature are based on large assumptions that may not hold true (Lesser 2013). This, together with the limitation of directly relating chlorophyll *a* fluorescence to photosynthesis, is why in the discussion below we will refer to our results as potentially implying that the relative light utilization may result in a shift in energy acquisition, but for a true measure, one would need to quantify all of the variables mentioned above.

The patterns of rETR distribution across different positions within an *A. humilis* colony, both in the deep and shallow, demonstrate that the outer side (side a, Fig. 1) of peripheral branches is likely to be light limited. The rETR mode of $10 \mu\text{mol e}^- \text{m}^{-2} \text{s}^{-1}$ found on the outer side of peripheral branches at both depths signifies that potential energy acquisition was low for these coral colony surfaces compared to all other within-colony branch surfaces. Inner branches within *A. humilis* colonies had higher modes of rETR levels at 50 and $75 \mu\text{mol e}^- \text{m}^{-2} \text{s}^{-1}$ rETR levels, and side b of outer branches had higher modes of rETR levels at $\geq 125 \mu\text{mol e}^- \text{m}^{-2} \text{s}^{-1}$ in the shallow and $\geq 50 \mu\text{mol e}^- \text{m}^{-2} \text{s}^{-1}$ in the deep. This implies potential for greater energy acquisition for these locations within *A. humilis* colonies at both depths. The overall high mode of rETR distribution at $10 \mu\text{mol e}^- \text{m}^{-2} \text{s}^{-1}$ found at both depths is probably a consequence of high levels of light attenuation within *A. humilis* colonies and can be due to branch self-shading within branching colonies. Despite evidence of minimizing light attenuation in deep compared to shallow environments (Kaniewska et al. 2008), the branching morphology is still strongly self-shaded. This may be due to genetic or environmental limitations to the extent to which branching corals can modify their colony structure. Although rETR is a relative estimate of electron flow through the photosystems (Ralph and Gademann 2005), it has been found that at low irradiance levels,

it approximates gross photosynthesis rate (Hoogenboom et al. 2006; Ulstrup et al. 2006) and the low rETR values obtained here may therefore represent reliable estimates of light utilization and photosynthetic rates.

Overall, colonies in the shallow had a higher whole-colony rETR, double that found in the deep. Due to a higher whole-colony rETR, colonies in the shallow have higher potential for light utilization and thus may also have higher potential for energy acquisition (Ralph et al. 2005). Colonies in the deep do not have the same light utilization potential and may in fact be approaching their ambient light limitation threshold at that depth. The depth limit for *A. humilis* colonies is 20 m at sites in the South Pacific Ocean (Wolstenholme et al. 2003). According to sensitivity analysis, branch position in a colony, that is the difference in outer versus inner branch coral surface incident light and chlorophyll *a* fluorescence, was the most influential parameter in estimating whole-colony rETR across the two depths. This most likely reflects the sun- and shade-adapted surface of the outer branches compared to the more uniform inner branch light climate where the only sun-adapted surface is the branch tip. The fact that whole-colony rETR is double that found in the deep is of particular interest since on chlorophyll *a* fluorescence parameters E_k and rETR_{max} found in this study were very similar across the two depths, that is there was no difference between depths (Tables 2, 3). This means that the difference in ambient light levels at each depth is what potentially drives this trend, as there is a fivefold difference in ambient light levels, yet the corals are photoacclimated to the same state at the two depths. Potentially the reason why corals from both depths are photoacclimated to the same state is that, overall in coral colonies at both depths, the modal whole-colony light level ($50 \mu\text{mol photons m}^{-2} \text{s}^{-1}$) was the same (Fig. 2). The difference between colonies at the two depths was that shallow corals had a higher frequency of coral surfaces exposed to light levels above $200 \mu\text{mol m}^{-2} \text{s}^{-1}$, and it may be that this is driving the difference in whole-colony rETR between the two depths. This also further confirms the sensitivity analysis, since the inner surface of the outermost branches (side b) would be exposed to the highest light levels thus potentially driving this difference together with the top part of inner branches. Our plotted values of F_0 (minimum fluorescence yield—dark-adapted) versus E/E_k also potentially indicate that shade-adapted surfaces on outer branches side b in shallow corals may have more pigmentation as the F_0 values were slightly higher. Also plotted NPQ values versus E/E_k also indicate there are differences between inner and outer branches where inner branches had higher NPQ values. This further strengthens the notion that branch position within a coral colony is influential in determining both the photoacclimatory state of the coral tissue and also its potential in determining whole-colony energy utilization.

Our results also suggest that comparisons of whole-colony rETR estimates show that photoacclimation via morphological variation in *A. humilis* found at 5 and 18 m may result in higher light utilization and therefore potentially higher energetic output. Simulations of whole-colony rETR estimates at deep ambient light levels revealed a higher rETR capacity for the deep type morphology model compared to the shallow type morphology model. These results indicate that phenotypic plasticity for this branching coral may shift energy acquisition across environmental gradients from an otherwise negative to a positive balance. Morphological variation in *A. humilis* does confer advantages for control of within-colony irradiance levels with changing ambient light levels. However, constraints from adopting a branching morphology may limit the degree of ‘openness’ possible in deep colonies. Comparing rETR capacity for type morphology models at 5 and 18 m for shallow ambient light levels reveals that rETR capacity was higher in the deep type morphology model. This could potentially indicate that the type morphology for colonies at 5 m may not maximize their light utilization and potential energy acquisition, but it may be that this type morphology reduces damaging impacts of photoinhibition. In support of this, inner branches of shallow colonies had higher values of NPQ when plotted against E/E_k (Fig. 4), which may indicate a greater investment into non-photochemical quenching mechanisms relative to inner branches found in deep corals (Henninge et al. 2008). Such an investment into photoacclimation could aid in protecting photosystem II reaction centres from excess excitation (Ralph and Gademann 2005).

It has been shown that energetic benefits from optimizing light harvesting can be outweighed by high costs of photoprotection (Hoogenboom et al. 2009). However, whole-colony rETR estimates derived in this study were only on a short-term temporal scale, and it has been demonstrated that short-term exposure to excessive light results in negligible costs for corals. Costs of photoinhibition and photodamage are not apparent until a time scale of days to weeks has been considered (Hoogenboom et al. 2006; Hoogenboom and Connolly 2009). Corals are likely to adapt to long-term average environmental conditions (Anthony et al. 2005). Therefore, although the type morphology present at 18 m could potentially increase light utilization and potential energetic acquisition at 5 m, as it had higher rETR, long-term effects and costs of photoinhibition may in fact result in overall lower potential energetic acquisition. Further investigation is required; testing photoacclimation of *A. humilis* coral surfaces at various ambient light levels on a larger time scale, to elucidate whether geometric variation at 5 m maximizes energy acquisition. It may also be that the *A. humilis* branching colony morphology is more important as a mechanism for maximizing surface area of living tissue relative to reef area than maximizing

energy acquisition per unit surface area (see also (Hoogenboom et al. 2008)). This is a common trend for many phenotypically plastic branching coral species, despite disadvantages such as reduction in potential for energy acquisition per unit surface area (Helmuth et al. 1997b; Muko et al. 2000; Sebens 1997). It has also been suggested that maximizing light utilization may be more important in low-light habitats for certain coral species (Hoogenboom et al. 2008). This may be the case for *A. humilis* where in the deep, low-light habitat; it may be more important to potentially maximize light utilization.

In conclusion, we show here that the pattern of both coral surface irradiance and rETR distribution is highly variable across a branching acroporid species common in shallow waters and that branch position is the most influential parameter in estimating whole-colony rETR. For *A. humilis*, phenotypic plasticity in terms of variation in colony morphology allows an overall shift of light utilization and potential energy acquisition across light regimes to a more positive balance. However, in highly lit shallow waters, potential energy acquisition is underutilized, which may be a result of the high costs of photoinhibition. Considering that this coral species is mostly abundant at shallow highly lit environments, this trade-off may prove cost beneficial as a long-term adaptation strategy for this particular niche.

Acknowledgments This work was supported by funding from the Australian Research Council and the University of Queensland. We thank N. Kongjandre, A. Gallenne and M. Stock for assistance with fieldwork. This is a contribution from the ARC Centre of Excellence for Coral Reef Studies.

References

- Achituv Y, Dubinsky Z (1990) Evolution and zoogeography of coral reefs. In: Dubinsky Z (ed) Ecosystems of the world 25. Coral Reefs. Elsevier, Amsterdam, pp 1–9
- Anthony KRN, Fabricius KE (2000) Shifting roles of heterotrophy and autotrophy in coral energetics under varying turbidity. *J Exp Mar Biol Ecol* 252:221–253
- Anthony KRN, Hoegh-Guldberg O (2003a) Variation in coral photosynthesis, respiration and growth characteristics in contrasting light microhabitats: an analogue to plants in forest gaps and understoreys? *Funct Ecol* 17:246–259
- Anthony KRN, Hoegh-Guldberg O (2003b) Kinetics of photoacclimation in corals. *Oecologia* 134:23–31
- Anthony KRN, Hoogenboom MO, Connolly SR (2005) Adaptive variation in coral geometry and the optimization of internal colony light climates. *Funct Ecol* 19:17–26
- Battery JF, Porter JW (1989) Photoadaptation as a whole organism response in *Montastrea annularis*. *Proc 6th Int Coral Reef Symp* 3:79–87
- Bradshaw AD (1965) Evolutionary significance of phenotypic plasticity in plants. *Adv Genet* 13:115–155
- Brown BE, Downs CA, Dunne RP, Gibb SW (2002) Exploring the basis of thermotolerance in the reef coral *Goniastrea aspera*. *Mar Ecol Prog Ser* 242:119–129

- Bruno JF, Edmunds PJ (1997) Clonal variation for phenotypic plasticity in the coral *Madracis mirabilis*. *Ecology* 78(7):2177–2190
- Bruno JF, Edmunds PJ (1998) Metabolic consequences of phenotypic plasticity in the coral *Madracis mirabilis* (Duchassaing and Michelotti): the effect of morphology and water flow on aggregate respiration. *J Exp Mar Biol Ecol* 229:187–195
- Chalker BE, Dunlap WC, Oliver JK (1983) Bathymetric adaptations of reef-building corals at Davies Reef, Great Barrier Reef, Australia. II. Light saturation curves for photosynthesis and respiration. *J Exp Mar Biol Ecol* 73:37–56
- Dove S (2004) Scleractinian corals with photoprotective host pigments are hypersensitive to thermal bleaching. *Mar Ecol Prog Ser* 272:99–116
- Dove S, Ortiz JC, Enriquez S, Fine M, Fisher P, Iglesias-Prieto R, Thornhill D, Hoegh-Guldberg O (2006) Response of holosymbiotic pigments from the scleractinian coral *Monipora monasteriata* to short-term heat stress. *Limnol Oceanogr* 51:1149–1158
- Dove S, Lovell C, Fine M, Deckenback J, Hoegh-Guldberg O, Iglesias-Prieto R, Anthony KRN (2008) Host pigments: potential facilitators of photosynthesis in coral symbioses. *Plant Cell Environ* 31:1523–1533
- Dubinsky Z, Falkowski PG, Porter JW, Muscatine L (1984) Absorption and utilization of radiant energy by light and shade-adapted colonies of the hermatypic coral *Stylophora pistillata*. *Proc R Soc Biol Sci Ser B* 222:203–214
- Dustan P (1979) Distribution of zooxanthellae and photosynthetic chloroplast pigments of the reef-building coral *Montastrea annularis* Ellis and Solander in relation to depth on a West Indian coral reef. *Bull Mar Sci* 29:79–95
- Enriquez S, Pantoja-Reyes NI (2005) Form-function analysis of the effect of canopy morphology on leaf self-shading in the seagrass *Thalassia testudinum*. *Oecologia* 145:235–243
- Enriquez S, Merino M, Iglesias-Prieto R (2002) Variations in the photosynthetic performance along the leaves of the tropical seagrass *Thalassia testudinum*. *Mar Biol* 140(5):891–900
- Enriquez S, Mendez ER, Iglesias-Prieto R (2005) Multiple scattering on coral skeletons enhances light absorption by symbiotic algae. *Limnol Oceanogr* 50:1025–1032
- Fagoonee I, Wilson HB, Hassell MP, Turner JR (1999) The dynamics of zooxanthellae populations: a long-term study in the field. *Science* 283(5403):843–845
- Falkowski PG, Dubinsky Z (1981) Light-shade adaptation of *Stylophora pistillata*, a hermatypic coral from the Gulf of Eliat. *Nature* 289:172–174
- Falkowski PG, Raven JA (1997) Aquatic photosynthesis. Blackwell Science, Malden, MA
- Fricke HW, Vareschi E, Schlichter D (1987) Photoecology of the coral *Leptoseris fragilis* in the Red Sea twilight zone (an experimental study by submersible). *Oecologia* 73:371–381
- Goulet TL, Coffroth MA (1997) A within colony comparison of zooxanthella genotypes in the Caribbean gorgonian *Plexaura kuna*. *Proc 8th Int Coral Reef Symp* 2:1331–1334
- Graus RR, Macintyre IG (1976) Light control of growth form in colonial reef corals: computer simulation. *Science* 193:895–897
- Hamby DM (1994) A review of techniques for parameter sensitivity analysis of environmental models. *Environ Monit Assess* 32:135–154
- Helmuth B, Timmerman BEH, Sebens KP (1997a) Interplay of host morphology and symbiont microhabitat in coral aggregation. *Mar Biol* 130:1–10
- Helmuth BS, Sebens KP, Daniel TL (1997b) Morphological variation in coral aggregations: branch spacing and mass flux to coral tissues. *J Exp Mar Biol Ecol* 209:233–259
- Henninge SJ, Smith DJ, Perkins R, Consalvey M, Paterson DM, Suggett DJ (2008) Photoacclimation, growth and distribution of massive coral species in clear and turbid waters. *Mar Ecol Prog Ser* 369:77–88
- Hill R, Schreiber U, Gademann R, Larkum A, Kuhl M, Ralph PJ (2004) Spatial heterogeneity of photosynthesis and the effect of temperature-induced bleaching conditions in three species of corals. *Mar Biol* 144:633–640
- Hoegh-Guldberg O, Jones RJ (1999) Photoinhibition and photoprotection in symbiotic dinoflagellates from reef-building corals. *Mar Ecol Prog Ser* 183:73–86
- Hood GM (2010) PopTools Version 3.2.5. Available at: <http://www.poptools.org>
- Hoogenboom MO, Connolly SR (2009) Defining fundamental niche dimensions of corals: synergistic effects of colony size, light, and flow. *Ecology* 90(3):767–780
- Hoogenboom MO, Anthony KRN, Connolly SR (2006) Energetic cost of photoinhibition in corals. *Mar Ecol Prog Ser* 313:1–12
- Hoogenboom MO, Connolly SR, Anthony KRN (2008) Interactions between morphological and physiological plasticity optimize energy acquisition in corals. *Ecology* 89(4):1144–1154
- Hoogenboom MO, Connolly SR, Anthony KRN (2009) Effects of photoacclimation on the light niche of corals: a process-based approach. *Mar Biol* 156(12):2493–2503
- Iglesias-Prieto R, Trench PK (1994) Acclimation and adaptation to irradiance in symbiotic dinoflagellates. I. Responses of the photosynthetic unit to changes in photon flux density. *Mar Ecol Prog Ser* 113:163–175
- Iglesias-Prieto R, Trench PK (1997) Acclimation and adaptation to irradiance in symbiotic dinoflagellates. II. Response of chlorophyll-protein complexes to different photon-flux densities. *Mar Biol* 130:23–33
- Jassby AD, Platt T (1976) Mathematical formulation of the relationship between photosynthesis and light for phytoplankton. *Limnol Oceanogr* 21(4):540–547
- Jokiel PL, Morrissey JI (1986) Influence of size on primary production in the reef coral *Pocillopora damicornis* and the macroalga *Acanthophora spicifera*. *Mar Biol* 91:15–26
- Jones RJ, Hoegh-Guldberg O, Larkum A, Schreiber U (1998) Temperature-induced bleaching of corals begins with impairment of the CO₂ fixation mechanism in zooxanthellae. *Plant, Cell Environ* 21:1219–1230
- Kaandorp JA, Sloot PMA, Merks RMH, Bak RPM, Vermeij MJA, Maier C (2005) Morphogenesis of the branching reef coral *Madracis mirabilis*. *Proc R Soc Biol Sci Ser B* 272(1559):127–133
- Kaniewska P, Anthony KRN, Hoegh-Guldberg O (2008) Variation in colony geometry modulates internal light levels in branching corals, *Acropora humilis* and *Stylophora pistillata*. *Mar Biol* 155(6):649–660
- Kaniewska P, Magnusson SH, Anthony KRN, Reef R, Kuhl M, Hoegh-Guldberg O (2011) Importance of macro-versus microstructure in modulating light levels inside coral colonies. *J Phycol* 47:846–860
- Kirk JTO (1994) Light and photosynthesis in aquatic ecosystems. Cambridge University Press, Cambridge
- Kleypas JA, McManus JW, Menez LAB (1999) Environmental limits to coral reef development: where do we draw the line? *Am Zool* 39:146–159
- Kuhl M, Cohen Y, Daalsgard T, Jorgensen BB, Revsbech NP (1995) Microenvironment and photosynthesis of zooxanthellae in scleractinian corals studied with microsensors for O₂, pH and light. *Mar Ecol Prog Ser* 117:159–172
- LaJeunesse TC, Loh WKW, van Woesik R, Hoegh-Guldberg O, Schmidt GW, Fitt WK (2003) Low symbiont diversity in southern great barrier reef corals, relative to those of the Caribbean. *Limnol Oceanogr* 48(5):2046–2054

- Lesser MP (2013) Using energetic budgets to assess the effects of environmental stress on corals: are we measuring the right things? *Coral Reefs* 32:25–33
- Lesser MP, Weis VM, Patterson MR, Jokiel PL (1994) Effects of morphology and water motion on carbon delivery and productivity in the reef coral, *Pocillopora damicornis* (Linnaeus): diffusion barriers, inorganic carbon limitation, and biochemical plasticity. *J Exp Mar Biol Ecol* 178(2):153–179
- Levy O, Dubinsky Z, Aчитuv Y (2003) Photobehavior of stony corals: responses to light spectra and intensity. *J Exp Biol* 206:4041–4049
- Marcelino LA, Westneat MW, Stoyneva V, Henss J, Rogers JD, Radosevich A, Turzitsky V, Siple M, Fang A, Swain TD, Fung J, Backman V (2013) Modulation of light-enhancement to symbiotic algae by light-scattering in corals and evolutionary trends in bleaching. *PLoS ONE* 8:e61492
- Mass T, Kline DI, Roopin M, Veal CJ, Cohen S, Iluz D, Levy O (2010) The spectral quality of light is a key driver of photosynthesis and photoadaptation in *Stylophora pistillata* colonies from different depths in the Red Sea. *J Exp Biol* 213:4084–4091
- Meyers LA, Bull JJ (2002) Fighting change with change: adaptive variation in an uncertain world. *Trends Ecol Evol* 17(12):551–557
- Muko S, Kawasaki K, Sakai K (2000) Morphological plasticity in the coral *Porites sillimaniani* and its adaptive significance. *Bull Mar Sci* 66:225–239
- Muscatine L, Porter JW (1977) Reef corals: mutualistic symbiosis adapted to nutrient-poor environments. *Bioscience* 27:454–460
- Oliver JK, Chalker BE, Dunlap WC (1983) Bathymetric adaptations of reef-building corals at Davies reef, Great Barrier Reef, Australia. I. Long-term growth responses of *Acropora formosa* (Dana 1846). *J Exp Mar Biol Ecol* 178:153–179
- Platt T, Gallegos CL, Harrison WG (1980) Photoinhibition of photosynthesis in natural assemblages of marine phytoplankton. *J Mar Res* 38:687–701
- Porter JW, Muscatine L, Dubinsky Z, Falkowski PG (1984) Primary production and photoadaptation in light- and shade-adapted colonies of the symbiotic coral, *Stylophora pistillata*. *Proc R Soc Biol Sci Ser B* 222:161–180
- Ralph PJ, Gademann R (2005) Rapid light curves: a powerful tool to assess photosynthetic activity. *Aquat Bot* 82:222–237
- Ralph PJ, Larkum AWD, Kuhl M (2005) Temporal patterns in effective quantum yield of individual zooxanthellae expelled during bleaching. *J Exp Mar Biol Ecol* 316(1):17–28
- Salih A, Larkum A, Cox G, Kuhl M, Hoegh-Guldberg O (2000) Fluorescent pigments in corals are photoprotective. *Nature* 408:850–853
- Sampayo EM, Franceschinis L, Hoegh-Guldberg O, Dove S (2007) Niche partitioning of closely related symbiotic dinoflagellates. *Mol Ecol* 16(17):3721–3733
- Sampayo EM, Ridgway T, Bongaerts P, Hoegh-Guldberg O (2008) Bleaching susceptibility and mortality of corals are determined by fine-scale differences in symbiont type. *P Natl Acad Sci USA* 105(30):10444–10449
- Sampayo EM, Dove S, Lajeunesse TC (2009) Cohesive molecular genetic data delineate species diversity in the dinoflagellate genus *Symbiodinium*. *Mol Ecol* 18(3):500–519
- Sebens KP (1997) Adaptive responses to water flow: morphology, energetics, and distribution of reef corals. *Proc 8th Int Coral Reef Symp* 2:1053–1058
- Silsbe GM, Kromkamp JC (2012) Modeling the irradiance dependency of the quantum efficiency of photosynthesis. *Limnol Oceanogr Method* 10:645–652
- Stambler N, Dubinsky Z (2005) Corals as light collectors: an integrating sphere approach. *Coral Reefs* 24:1–9
- Stimson J (1997) The annual cycle of density of zooxanthellae in the tissues of field and laboratory-held *Pocillopora damicornis* (Linnaeus). *J Exp Mar Biol Ecol* 214:35–48
- Sultan SE, Spencer HG, Schmitt JM (2002) Metapopulation structure favors plasticity over local adaptation. *Am Nat* 160(2):271–283
- Titlyanova EA, Titlyanova TV, van Woesik R, Yamazato K (2002) Acclimation of the hermatypic coral *Stylophora pistillata* to bright light. *Russ J Mar Biol* 28(Supplement 1):S41–S46
- Ulstrup KE, Berkelmans R, Ralph PJ, van Oppen MJH (2006) Variation in bleaching sensitivity of two coral species across a latitudinal gradient on the Great Barrier Reef: the role of zooxanthellae. *Mar Ecol Prog Ser* 314:135–148
- Vermeij MJA, Bak RPM (2002) How are coral populations structured by light? Marine light regimes and the distribution of *Madracis*. *Mar Ecol Prog Ser* 233:105–116
- Via S, Gomulkiewicz R, De Jong G, Scheiner SM, Schlichting CD, Van Tienderen PH (1995) Adaptive phenotypic plasticity: consensus and controversy. *Trends Ecol Evol* 10(5):212–217
- Wangpraseurt D, Larkum AWD, Ralph PJ, Kuhl M (2012) Light gradients and optical microniches in coral tissues. *Front Microbiol* 3:316
- Warner WEC, Chilcoat G, McFarland FK, Fitt KW (2002) Seasonal fluctuations in the photosynthetic capacity of photosystem II in symbiotic dinoflagellates in the Caribbean reef-building coral *Montastrea*. *Mar Biol* 141:31–38
- Willis BL (1985) Phenotypic plasticity versus phenotypic stability in the reef corals *Turbinaria mesenterina* and *Pavona cactus*. *Proc 5th Int Coral Reef Symp* 4:107–112
- Wolstenholme JK, Wallace CC, Chen CA (2003) Species boundaries within the *Acropora humilis* species group (Cnidaria; Scleractinia): a morphological and molecular interpretation of evolution. *Coral Reefs* 22(2):155–166